THE JOURNAL OF BIOLOGICAL CHEMISTRY VOL. 284, NO. 37, pp. 25004–25014, September 11, 2009

Mitochondrial Glutamate Carrier GC1 as a Newly Identified Player in the Control of Glucose-stimulated Insulin Secretion*

Received for publication, April 30, 2009 Published, JBC Papers in Press, July 7, 2009, DOI 10.1074/jbc.M109.015495

Marina Casimir[‡], Francesco M. Lasorsa[§], Blanca Rubi[‡], Dorothée Caille[‡], Ferdinando Palmieri[§], Paolo Meda[‡], and Pierre Maechler[‡1]

From the [‡]Department of Cell Physiology and Metabolism, Faculty of Medicine, University of Geneva, 1 Rue Michel-Servet, 1211 Geneva 4, Switzerland and the [§]Department of Pharmaco-Biology, Laboratory of Biochemistry and Molecular Biology, University of Bari, and CNR Institute of Biomembranes and Bioenergetics, Via E. Orabona 4, 70125 Bari, Italy

The SLC25 carrier family mediates solute transport across the inner mitochondrial membrane, a process that is still poorly characterized regarding both the mechanisms and proteins implicated. This study investigated mitochondrial glutamate carrier GC1 in insulin-secreting β-cells. GC1 was cloned from insulin-secreting cells, and sequence analysis revealed hydropathy profile of a six-transmembrane protein, characteristic of mitochondrial solute carriers. GC1 was found to be expressed at the mRNA and protein levels in INS-1E β-cells and pancreatic rat islets. Immunohistochemistry showed that GC1 was present in mitochondria, and ultrastructural analysis by electron microscopy revealed inner mitochondrial membrane localization of the transporter. Silencing of GC1 in INS-1E β-cells, mediated by adenoviral delivery of short hairpin RNA, reduced mitochondrial glutamate transport by 48% ($p < 0.001$). Insulin secretion at basal 2.5 mM glucose and stimulated either by intermediate 7.5 mM glucose or non-nutrient 30 mM KCl was not modified by GC1 silencing. Conversely, insulin secretion stimulated with optimal 15 mM glucose was reduced by 23% ($p < 0.005$) in GC1 knocked down cells compared with controls. Adjunct of cell-permeant glutamate (5 mM dimethyl glutamate) fully restored the secretory response at 15 mM glucose ($p < 0.005$). Kinetics of insulin secretion were investigated in perifused isolated rat islets. GC1 silencing in islets inhibited the secretory response induced by 16.7 mM glucose, both during first (−25%, $p < 0.05$) and second (−33%, $p < 0.05$) phases. This study demonstrates that insulin-secreting cells depend on GC1 for maximal glucose response, thereby assigning a physiological function to this newly identified mitochondrial glutamate carrier.

Functions of mitochondria require regulated flux of molecules across the two membranes surrounding the matrix. Mitochondrial solute carriers (SLC25) are a large family of nuclearly encoded membrane-embedded proteins that promote solute transport across the inner mitochondrial membrane (1–4). The human genome contains 48 members of the SLC25 family, among them about 30 have been identified and characterized biochemically (1, 5–8). In particular, very little is known on solute carrier proteins transporting metabolites, such as glutamate. The two isoforms of the glutamate carrier GC1 and GC2 (encoded by SLC25A22 and SLC25A18, respectively) catalyze the transport of glutamate across the inner mitochondrial membrane, either by proton co-transport or in exchange for hydroxyl ions. To date, one human pathology has been associated with GC1, exhibiting a correlation between GC1 mutation and neonatal myoclonic epilepsy (9). Of interest, the high K_m isoform GC1 was shown to be expressed in different tissues, especially in the brain, liver, and pancreas (10). Despite the importance of these studies, we still lack subcellular localization and demonstration of the physiological function of glutamate carriers. The elevated expression levels in the pancreas triggered our interest, given that the glutamate pathway has been highlighted over the last years in the endocrine pancreas in general and the β-cell in particular (11). Still, the putative mechanisms responsible for mitochondrial glutamate transport have not yet been characterized in specialized tissues such as insulin-secreting cells. Only two carriers involved in mitochondrial shuttles have been shown to play an important role in the control of insulin secretion, *i.e.* the aspartate/glutamate carrier (AGC1 or Aralar1) (12) and the citrate/isocitrate carrier (13).

It is well founded that mitochondrial metabolism is crucial in pancreatic β-cells by generating signals involved in metabolism-secretion coupling (14). Upon glucose stimulation, generation of ATP through mitochondrial activation leads to the closure of ATP-sensitive K^+ channels and depolarization of the plasma membrane (15). This, in turn, induces the opening of voltage-dependent calcium channels resulting in elevation of cytosolic Ca^{2+} (16). Ca^{2+} is necessary but not sufficient for the full development of the insulin secretory response (17). Other messengers have been proposed to contribute to stimulation of insulin exocytosis, such as protein kinases A and C, long chain acyl-CoAs, nucleotides, and glutamate (18). The involvement of the latter amino acid was deduced from experiments performed under conditions of intracellular [Ca^{2+}] clamped at permissive concentrations, during which intracellular provision of glutamate directly stimulated insulin exocytosis (19–21). Based on these results, it was proposed that glutamate could act downstream of mitochondrial function, participating in the coupling of glucose metabolism to insulin secretion (21).

* This work was supported by the Swiss National Science Foundation (to P. Maechler and P. Meda), the European Foundation for the Study of Diabetes/Novo Nordisk research grant (to P. Maechler), the Novartis Foundation (to P. Maechler), Novo Nordisk (P. Meda), the Ministero dell'Università e della Ricerca (to F. P.) and Apulia Region (to F. P.), the Juvenile Diabetes Research Foundation (P. Meda), and the European Union (P. Meda). This study was part of the Geneva Programme for Metabolic Disorders.

[1] To whom correspondence should be addressed. Tel.: 41-22-379-55-54; E-mail: Pierre.Maechler@unige.ch.

The importance of the glutamate pathway for β-cell function is illustrated in transgenic mice (named *βGlud1*$^{-/-}$) with conditional β-cell-specific deletion of the mitochondrial enzyme glutamate dehydrogenase, resulting in about 40% reduction of glucose-stimulated insulin secretion (22). The exact role of glutamate in β-cell function is still debated as the glutamate pathway might raise insulin release by participating in the amplifying pathway (19–21) and/or by relaying signals of protein abundance to mitochondria (23–25). In both models, glutamate should be transported in and out of the mitochondria by some putative mitochondrial carrier that remains to be identified in β-cells. Overall, better characterization of mitochondrial glutamate handling will contribute to our comprehension of mechanisms implicated in the control of insulin secretion.

In this study, we identified glutamate carrier GC1 as being expressed in the inner mitochondrial membrane of insulinoma INS-1E cells as well as in primary rat islets. Adenovirus-mediated knockdown of GC1 by shRNA[2] demonstrated physiological functionality of GC1 in insulin secretion.

EXPERIMENTAL PROCEDURES

Cell Culture—Clonal INS-1E cells (26), derived from the parental rat insulinoma INS-1 cell line, were cultured in a humidified atmosphere with 5% CO_2 in complete RPMI 1640 medium supplemented with 5% heat-inactivated fetal calf serum, 1 mM sodium pyruvate, 50 μM 2-mercaptoethanol, 2 mM glutamine, 10 mM HEPES, 100 units/ml penicillin, and 100 μg/ml streptomycin. Rat islets were isolated from adult male Wistar rats by collagenase perfusion (27) and cultured in complete RPMI 1640 medium. HEK 293 cells were cultured in Dulbecco's modified Eagle's medium supplemented with 5% fetal calf serum and the penicillin/streptomycin antibiotics.

Expression Analysis of GC1 in INS-1E Cells and Rat Islets—Total RNA was extracted from INS-1E cells and rat islets, and the reverse transcription was performed using 2 μg of total RNA, mediated by the enzyme SuperScript II (Invitrogen). The PCR program for cDNA was as follows: initial denaturation step at 94 °C for 2 min, 40 cycles of denaturation at 94 °C, annealing at 60 °C, and elongation at 72 °C, for 1 min each. A final elongation step of 7 min at 72 °C allowed extension of truncated product to full length. PCRs were performed using *Taq*DNA polymerase (Amersham Biosciences) with 1.5 μM concentrations of each primer. Several primers designed from the mice *GC1* ortholog (accession number AK010193) were tested, and multiple PCRs followed by sequencing were performed to determine the putative open reading frame for rat *GC1*. With the resulting sequence, we designed primers flanking the open reading frame, to obtain the full-length *GC1* cDNA fragment. The forward and reverse primers used for the amplification of the open reading frame were as follows: 5′-GGC CTG ACT CCT GCT TCA CTT GGT GTA A-3′ and 5′-GGC CTG GGG TTC TTG CAG CAG-3′. As positive control, we used primers designed to amplify the housekeeping gene cyclophilin (5′-GGT CAA CCC CAC CGT GTT CT-3′ and 5′-TGC-CATCCAGCCACTCAGTCT for sense and antisense primer sequence, respectively). Negative control PCRs were performed with *GC1* primers on INS-1E and rat islet RNA that were not reverse-transcribed (−RT).

shRNA Design and Adenovirus Generation—Two small interfering RNA constructs were designed from the rat *GC1* cDNA sequence as a hairpin-loop structure using the Ambion website tool (small interfering RNA Target Finder). These constructs were tested by cloning into a pSilencer plasmid, and their potency was assessed by performing Lipofectamine (Invitrogen)-mediated transfection and immunoblotting. The most efficient shRNA cassette (5′-GCTGGCTGCTAATGAC-TTCTTCAAGAGAGAAGTCATTAGCAGCCAGCTTTTT-TGGAA-3′ and 5′-CGTTCCAAAAAAGCTGGCTGCTAAT-GACTTCTCTCTTGAAGAAGTCATTAGCAGCCAGCG-GCC-3′), along with the U6 promoter, was excised. Klenow reaction was performed to create blunt ends, and the resulting insert was then subcloned in a promoterless recombinant adenovirus that was previously opened with SwaI. The resulting construct was first sequenced to check for the occurrence of mutations prior to co-transfection using the calcium-phosphate method in HEK293 cells along with the adenovirus DNA-terminal protein complex. Ten days after transfection, the cell lysate was used to infect cells in 24-well plates, and the adenoviral DNA was extracted from the cells and analyzed by DNA digestion with ClaI and EcoRI to check for the presence of the insert and for its orientation, respectively. The virus was then amplified and purified as described previously (12).

Adenovirus-mediated Transduction—Unless otherwise mentioned, adherent cultures of INS-1E cells were transduced with recombinant adenoviruses at a viral titer of ~30 plaque-forming units/ml for 1 h at 37 °C, and experiments were performed 4 days after transduction. An empty adenoviral construct used at the same titer served as control and was referred to as Empty control. Transduction of rat islets was performed on the day of isolation at a titer of 60 plaque-forming units/ml for 90 min, as determined previously for efficient islet cell transduction (12, 27). As for INS-1E cells, experiments were performed 4 days post-transduction.

Mitochondrial Isolation—Cells seeded in 15-cm Petri dishes (10^6 cells/dish) were transduced with Empty and AdshGC1 adenoviruses 4 days before fractionation. The cells were then washed with ice-cold phosphate-buffered saline, collected by scraping in 250 mM sucrose, 20 mM Tris/HCl, pH 7.4, supplemented with 0.5% BSA. Mitochondria were fractionated by Potter-Elvehjem homogenization and serial centrifugations as described previously (28). The mitochondrial pellet was resuspended in lysis buffer for immunoblotting analysis.

Immunoblotting and Immunoprecipitation—For detection of GC1 at the protein level, an antibody directed against rat GC1 was raised in a rabbit using the peptide sequence CDVVKTRLQSERGVN corresponding to amino acids 246–261 as synthetic antigen (Eurogentec, Seraing, Belgium). Generation of the antiserum was performed using a standard immunization program. After four serial injections of the peptide, blood was taken at different time points, with the final bleeding 3 months after the first peptide injection. Serum resulting from the final bleeding was first tested by

[2] The abbreviations used are: shRNA, short hairpin RNA; BSA, bovine serum albumin; RT, reverse-transcribed; FCCP, carbonyl cyanide *p*-trifluoromethoxyphenylhydrazone; PIPES, 1,4-piperazinediethanesulfonic acid.

enzyme-linked immunosorbent assay, and the condition that was used for GC1 detection was optimized by testing different dilutions of the anti-GC1 serum. Serum obtained from the blood sample that was taken before immunization was referred to as preimmune and used in our experiments as a background control for GC1 immunodetection.

The specificity of the antiserum raised against GC1 was tested using recombinant GC1 and GC2 proteins that were expressed and purified as described previously (10). Purified GC1 and GC2 isoforms at different concentrations were subjected to a 15% SDS-PAGE and then transferred onto nitrocellulose membrane. Incubation with GC1 antiserum was performed overnight at 4 °C in blocking buffer (12) containing the anti-GC1 antiserum (1:1000). The following day, the membrane was probed for 2 h at room temperature with donkey anti-rabbit IgG antibody (1:5000) conjugated to horseradish peroxidase (ECL, Amersham Biosciences), and GC1 protein was revealed by chemiluminescence (Pierce).

Similar immunoblotting protocol was performed to determine the expression of GC1 in different protein extracts from INS-1E cells. Therefore, total cell extracts or mitochondrion-enriched fractions were first lysed in a buffer containing 0.1 M EDTA, 0.1 M EGTA, β-mercaptoethanol, 20% Triton X-100 diluted in Tris/HCl, pH 7.4, supplemented with 1 mM phenylmethylsulfonyl fluoride and subjected to a 15% SDS-polyacrylamide gel. Immunoblotting analysis was performed as described previously.

Where mentioned, immunoblotting analyses were performed following an additional step used for clearance of unspecific proteins recognized by the preimmune serum. Specifically, immunoprecipitation was performed on cell extracts, and the resulting supernatant was subjected to immunoblotting. For immunoprecipitation, cells were lysed at 4 °C in a buffer containing 10 mM Tris/HCl, pH 7.6, 150 mM NaCl, 1% Triton X-100, 0.1% SDS, 2 mM EDTA, 1% sodium deoxycholate, and protease inhibitors (RIPA buffer). A total of 600 μg of proteins were incubated overnight with 20 μl of preimmune antiserum under agitation at 4 °C. This was performed as an additional pre-clearing step to prevent unspecific binding of proteins to A/G-Sepharose beads. Immune complexes were precipitated with the beads and washed extensively before collecting supernatants. The resulting supernatants were incubated with 10 μl of anti-GC1 serum overnight at 4 °C. The following day, immune complexes were again precipitated, and after five serial washes, complexes were dissociated at 95 °C for 5 min with Laemmli loading buffer, and the supernatant was collected for immunoblot analysis.

Immunohistochemistry—INS-1E cells were seeded on poly-ornithine-treated glass coverslips 3 days prior to infection with empty or AdshGC1 viruses. Four days post-transduction, cells were incubated with Mitotracker, fixed with cold methanol, and permeabilized as described previously (29). The slides were then incubated with anti-GC1 and preimmune sera (1:500) overnight at 4 °C. The following day, after several washes with phosphate-buffered saline, samples were exposed to secondary antibody goat anti-rabbit IgG fluorescein isothiocyanate (1:200, Chemicon AP132F, Temecula, CA) for 1 h at room temperature. Coverslips were then mounted on glass slides, and samples were analyzed using a ×63 objective in Axiocam microscope (Zeiss, Zürich, Switzerland). Acquisition times were kept the same between groups according to channels to compare signal intensities.

Immunoelectron Microscopy—Pellets of control and AdshGC1-transduced INS-1E cells, either total or mitochondrial enriched, were washed twice in 0.1 M phosphate buffer, before a 60-min fixation at room temperature in 4% paraformaldehyde or a 5-min fixation in 4% paraformaldehyde plus 0.1% glutaraldehyde, followed by a 55-min fixation in 4% paraformaldehyde alone (all fixatives diluted in 0.1 M phosphate buffer, pH 7.4). The samples were then frozen and thin-sectioned with an EMFCS cryo-ultramicrotome (Leica). The sections were mounted on parlodion-coated copper grids and incubated as described (30, 31). Briefly, the glutamate transporter GC1 was immunolabeled for 1 h at room temperature using the GC1-specific antiserum, diluted 1:40–50. Antigen-antibodies complexes were revealed after a 20-min incubation at room temperature with either 15 nm gold particles coated with protein A or a goat anti-rabbit IgG serum coupled to 10 nM gold particles (British Biocell International, Cardiff, Wales) diluted 1:10. In all incubations, controls included exposure of the sections to either the preimmune serum, as well as incubations with only the protein A-coated gold particles or the gold-conjugated goat antibodies.

NAD(P)H Measurements—NAD(P)H generation was assessed in Empty and AdshGC1-transduced cells stimulated with 15 mM glucose, after stabilization of the signal for 10 min in Krebs-Ringer bicarbonate HEPES buffer (KRBH, containing in mM: 135 NaCl, 3.6 KCl, 10 HEPES, pH 7.4, 5 $NaHCO_3$, 0.5 NaH_2PO_4, 0.5 $MgCl_2$, 1.5 $CaCl_2$). NAD(P)H recordings were performed using a thermostated plate reader (Fluostar Optima, BMG Labtechnologies, Offenburg, Germany), and autofluorescence was measured using excitation and emission filters set at 340 and 470 nm, respectively. NAD(P)H autofluorescence was normalized over a 10-min stimulation period by setting the fluorescence at 100% for cells maintained in basal 2.5 mM glucose.

Mitochondrial Membrane Potential—Mitochondrial membrane potential ($\Delta\Psi_m$) was measured using the fluorescent probe rhodamine-123 as described previously (26). INS-1E cells were cultured in 24-well plates and isolated islets in 96-well plates and maintained in KRBH with 2.5 mM glucose supplemented sequentially during the recording with the indicated substrates, and then 1 μM of the protonophore carbonyl cyanide *p*-trifluoromethoxyphenylhydrazone (FCCP) was added.

Cytosolic ATP Measurements—Cytosolic ATP levels were monitored in a thermostated plate reader (Fluostar Optima) on control and AdshGC1-treated cells in the presence of 100 μM beetle luciferin (Promega Corp., Madison, WI). The day before the experiment, cells were transduced with the AdCAG-Luciferase viral construct enabling expression of the ATP-sensitive bioluminescent probe luciferase (26, 32). Changes in luminescence, reflecting cytosolic ATP levels, were monitored at basal 2.5 mM glucose before stimulation during 20 min with 15.5 mM glucose followed by the addition of the mitochondrial poison azide (2 mM).

Cellular Ca^{2+} Levels—Cytosolic Ca^{2+} changes were monitored as detailed previously (33) in cells preincubated for 90

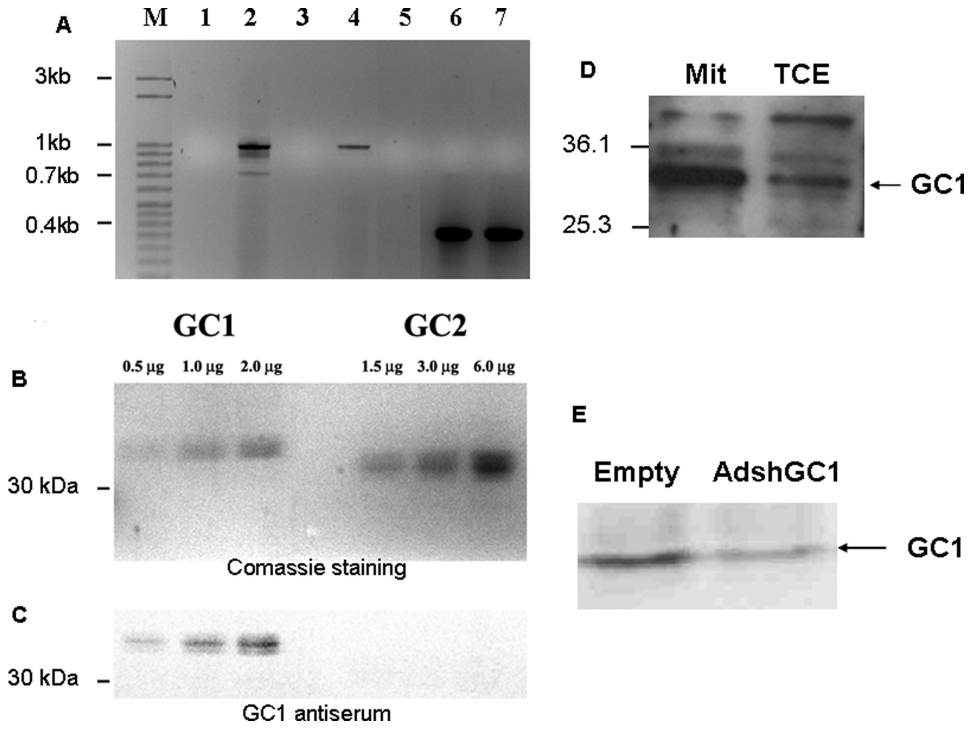

FIGURE 1. **GC1 expression analysis in INS-1E β-cells and rat islets.** *A*, RT-PCR analysis on cDNA from INS-1E cells and rat islets using primers designed to amplify the open reading frame of GC1 and cyclophilin as housekeeping gene. *M*, 50-bp marker; *lane 1*, negative control (*i.e.* PCR mix without enzyme); *lane 2*, GC1 in INS-1E cDNA; *lane 3*, GC1 in INS-1E cDNA minus RT; *lane 4*, GC1 in rat islet cDNA; *lane 5*, GC1 in rat islet cDNA minus RT; *lane 6*, cyclophilin in INS-1E cDNA; *lane 7*, cyclophilin in rat islet cDNA. *B* and *C*, evaluation of the specificity of GC1 antiserum. Purified recombinant isoforms GC1 (0.5, 1.0, and 2 μg) and GC2 (1.5, 3.0, and 6.0 μg) were loaded on 15% SDS-PAGE. Proteins were visualized by Coomassie staining (*B*) and then transferred onto nitrocellulose membrane for immunodetection with the GC1 antiserum (*C*). *D*, immunoblot analysis of GC1 expression following SDS-PAGE 15% protein separation using 40 μg of proteins per lane. *Mit*, INS-1E mitochondrion-enriched fractions; *TCE*, INS-1E total cell extracts. *E*, immunoblot following an immunoprecipitation using preimmune serum. GC1 expression in INS-1E cells transduced either with control Empty adenovirus or with AdshGC1 to test efficiency of the shRNA construct was analyzed.

min with 2 μM Fura-2AM (Teflab, Austin, TX) in KRBH at 37 °C and then washed before the experiment. Ratiometric measurements of Fura-2 fluorescence were performed in a plate reader fluorimeter (Fluostar Optima) with filters set at 510 nm for excitation and 340/380 nm for emission.

Glutamate Transport Activity—Isolated mitochondria from transduced INS-1E cells (0.5 mg/ml) were solubilized in a buffer containing 3% Triton X-114, 1 mM EDTA, 20 mM Na_2SO_4, and 10 mM PIPES, pH 7.0, for 30 min at 0 °C (34). 20 μg of solubilized mitochondria were reconstituted into liposomes in the presence of L glutamate or L-aspartate (35). External substrate was removed from proteoliposomes on Sephadex G-75 columns, pre-equilibrated with 50 mM NaCl, 1 mM EDTA, and 10 mM PIPES, pH 7.0. Transport at 25 °C was started by the addition of L-[U-^{14}C]glutamate (10) or L-[U-^{14}C]aspartate (36) and terminated by addition of 15 mM pyridoxal 5′-phosphate and 10 mM bathophenanthroline (35). In controls, the inhibitors were added at the beginning together with the external substrate. Finally, the external substrate was removed, and the radioactivity in the proteoliposomes was measured. The experimental values were corrected by subtracting control values (35).

Insulin Secretion Assay on INS-1E Cells—Secretory responses to the indicated secretagogues were tested in INS-1E cells transduced with Empty control and AdshGC1 viruses. Before the experiments, cells were maintained for 2 h in 2.5 mM glucose RPMI 1640 medium. Cells were then washed and preincubated for 30 min in glucose-free KRBH containing 0.1% BSA as insulin carrier. Finally, cells were stimulated for 30 min in KRBH-BSA with increasing glucose concentrations (basal 2.5 mM, intermediate 7.5 mM, and optimal 15 mM glucose) (26). Cells were also exposed to 15 mM glucose in the presence of 5 mM dimethyl glutamate for rescue tests. Non-nutrient-stimulated insulin release was evoked by the calcium-raising agent KCl (30 mM) at basal 2.5 mM glucose. Insulin concentrations were measured using radioimmunoassay kits (Linco Research, St. Charles, MO).

Insulin Secretion Assay on Rat Islets—Islet perifusions were carried out as described (27) using 10 hand-picked islets per chamber of 250 μl volume at 37 °C (Brandel, Gaithersburg, MD). The KRBH-BSA flux was set at 0.5 ml/min, and fractions were collected every min after a 30-min washing period at basal 2.8 mM glucose. Basal 2.8 mM glucose was kept for 20 min and then raised to 16.7 mM for 20 min. First and second phases of insulin secretion were analyzed as minutes 1–5 and 6–10 after glucose stimulation (16.7 mM), respectively. Quantification of insulin release over phase periods was expressed as area under the curves.

Statistics—Unless otherwise indicated, data are the means ± S.E. of at least three independent experiments, each performed in quadruplicate. Differences between groups were assessed by the Student's *t* test for paired data and by one-way analysis followed by Bonferroni *t* test as mentioned.

RESULTS

Detection of GC1 in INS-1E β-Cells and Rat Islets—We first investigated the expression of GC1 in insulin-secreting cells. This was achieved both in rat insulinoma INS-1E cells and isolated rat pancreatic islets. To this end, primers designed from mouse GC1 cDNA sequence were chosen to amplify rat cDNA from both INS-1E and rat islets. PCR bands revealed an open reading frame of 978 bp in length (Fig. 1*A*). Although expression of the glutamate carrier GC2 isoform was previously found to be low in the whole pancreas (10), we checked messenger levels by quantitative RT-PCR. GC2 expression was undetectable in INS-1E cells as opposed to positive control obtained from rat brain mRNA (data not shown).

BLAST analysis against the human and mouse GC1 sequences gave similarity scores of 96 and 98%, respectively. In addition, BLAST analysis against the rat genome data base

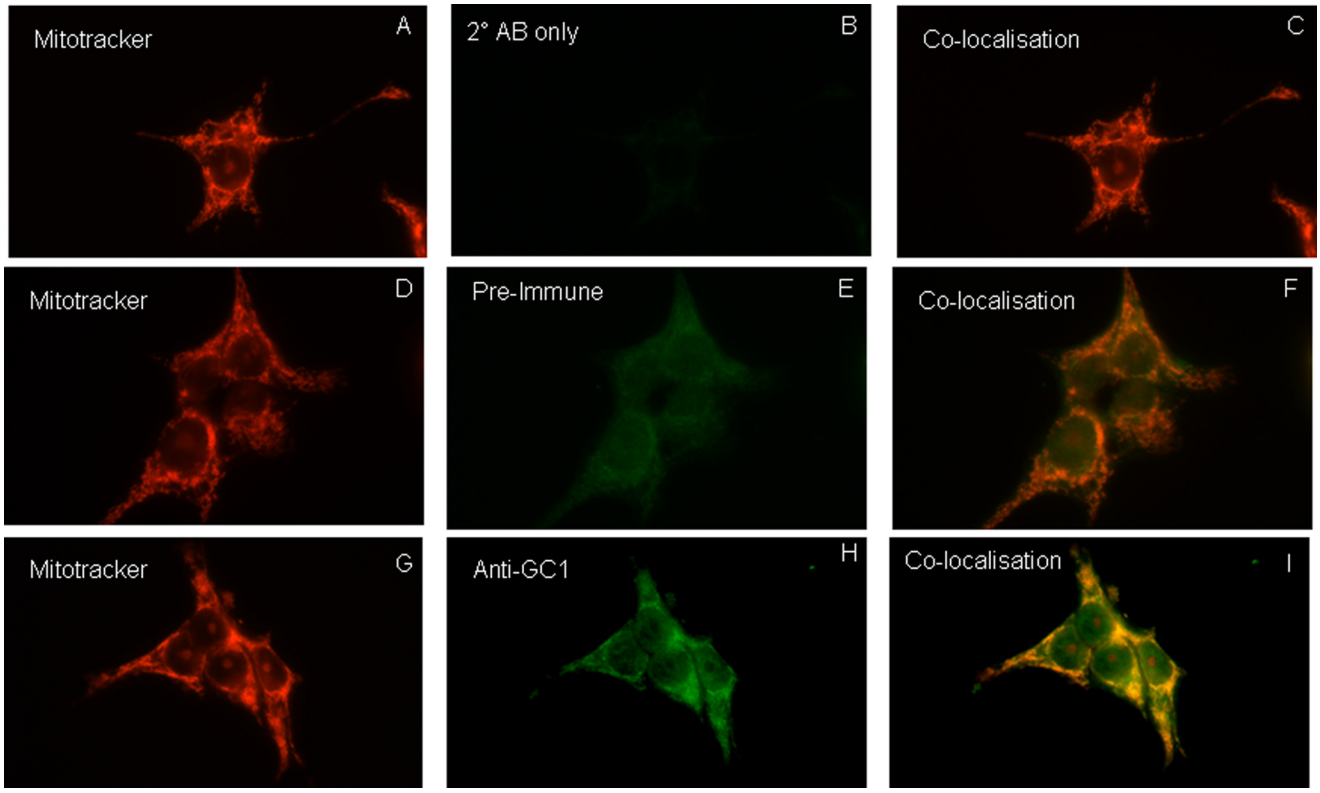

FIGURE 2. **Localization of GC1 at the cellular level by immunofluorescence.** Immunolocalization of GC1 in INS-1E cells by staining mitochondria using Mitotracker (*A*, *D*, and *G*) and GC1 using GC1 antiserum (*H*) plus fluorescein isothiocyanate-conjugated secondary antibody (*B*, *E*, and *H*). Preimmune serum was used as negative control (*E*). *A–C*, control INS-1E cells without GC-1 antiserum. *D–F*, control INS-1E cells using preimmune serum. *G–I*, control INS-1E cells. Images are representative of 5–6 independent experiments.

revealed 100% homology with the INS-1-derived sequence, which corresponds to one of the BACs NW_001084774 of the rat genome library. These results show that this newly identified gene corresponds to the rat GC1, and the 100% sequence similarity confirms sequence conservation and accuracy. Bioinformatics analysis showed that the sequenced GC1 exhibited the main characteristics of all mitochondrial solute carriers, *i.e.* hydropathy profile of a six-transmembrane protein and the presence of a 3-fold repeated signature motif (data not shown).

Detection of GC1 at the protein level was performed with an antibody directed against the peptide sequence corresponding to amino acids 246–261 of GC1. First, specificity of GC1 antiserum was assessed by immunoblotting using purified recombinant GC1 and GC2 isoforms on SDS-PAGE (Fig. 2, *B* and *C*). Coomassie staining showed both GC1 and GC2 bands (Fig. 2*B*), although GC1 antiserum detected only the GC1 isoform (Fig. 1*C*), thereby demonstrating its specificity.

Next, expression of GC1 in both INS-1E total cell extracts and mitochondria-enriched fractions was evaluated. Immunoblotting revealed an immunoreactive band within the predicted GC1 size range between molecular mass markers 25 and 36 kDa. This band was markedly enriched in mitochondrial preparations compared with total cell extracts (Fig. 1*D*). In contrast, faint unspecific bands observed at sizes not compatible with GC1 were lower in mitochondrial fractions compared with total cell extracts. Similar unspecific bands were also revealed using preimmune serum (data not shown). To test if such extra bands were indeed unspecific, *i.e.* recognized by preimmune serum, we performed an additional preclearing step whereby cell extracts were subjected to an immunoprecipitation using preimmune serum. The resulting supernatant was used to run an immunoblot with GC1 antiserum showing a unique 32-kDa band identified as GC1 protein (Fig. 1*E*).

To reduce GC1 expression, INS-1E cells were treated with an adenovirus construct (AdshGC1) designed to down-regulate GC1. Cells analyzed by immunoblotting 4 days after AdshGC1 transduction exhibited reduced expression of the identified GC1 protein compared with cells treated with control empty adenovirus (Fig. 1*E*). Incidentally, this maneuver further assessed the specificity of the antiserum. Densitometry analysis indicated a reduction of ~70% in GC1 protein levels 4 days after AdshGC1 treatment. Mitochondrial membrane protein half-life is poorly characterized, with an estimate of about 24 h (37). One can extrapolate that 4 days after transduction with AdshGC1 less than 90% of the initial GC1 protein pool should be left, giving an approximate efficiency of 60% for shRNA-mediated knockdown. Silencing of GC1 did not induce compensatory GC2 expression as this latter isoform remained undetectable by quantitative RT-PCR (data not shown).

Cellular and Ultrastructural Localization of GC1—Immunofluorescence studies were conducted in INS-1E cells for subcellular localization of GC1 (Fig. 2). Incubation of fixed cells with preimmune serum or with only secondary antibody exhibited weak background staining. Conversely, keeping fluorescence gain of function at the same level, GC1 antiserum gave rise to a strong signal exhibiting mitochondrial pattern. The anti-GC1

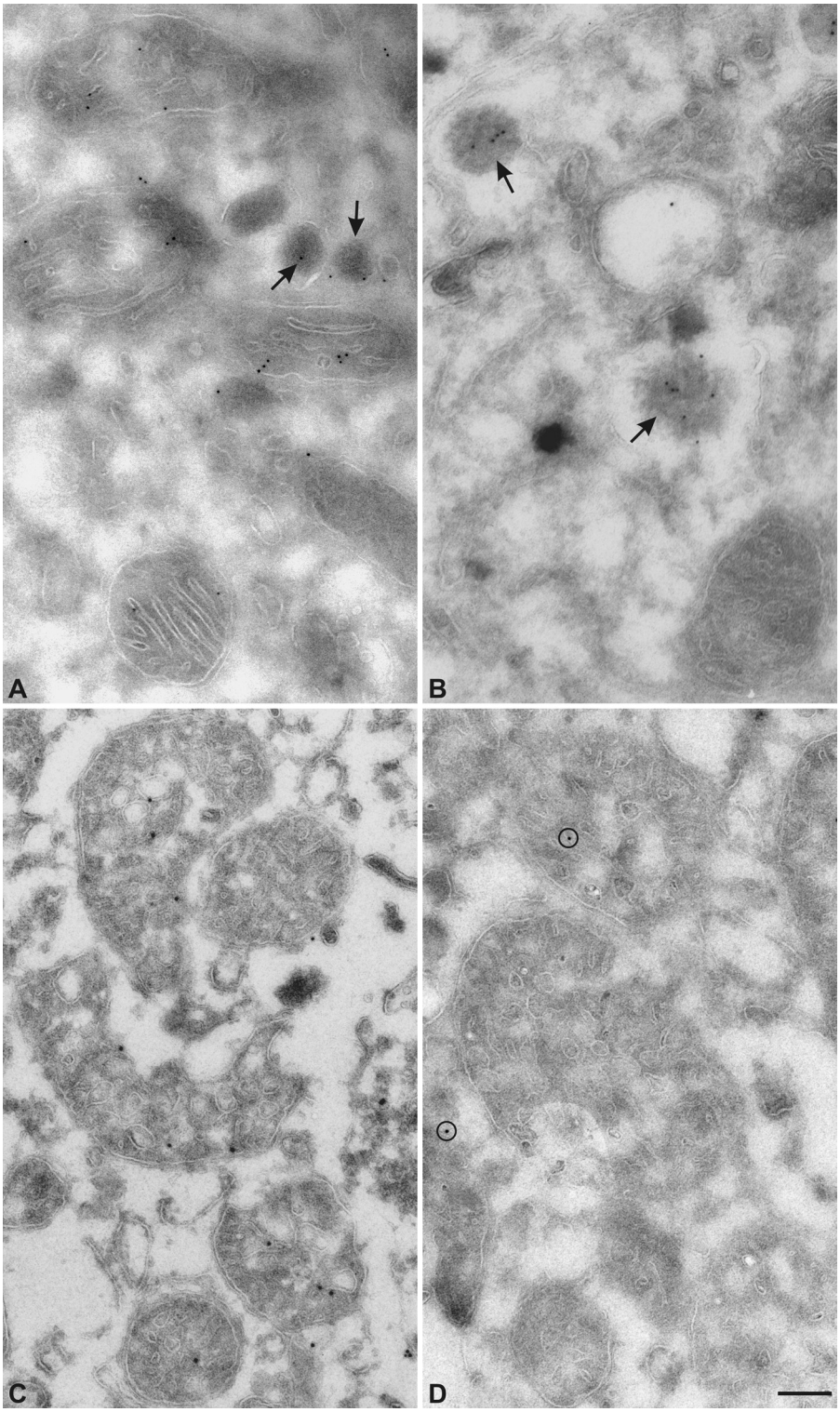

FIGURE 3. **Localization of GC1 at the ultrastructural level by electron microscopy.** *A,* immunolabeling of INS-1E cells using GC1 antiserum. *B,* immunolabeling of INS-1E cells using preimmune serum as negative control. *C,* immunolabeling on mitochondrial preparation from INS-1E cells using GC1 antiserum. *D,* AdshGC1-mediated GC1 down-regulation in INS-1E cells 4 days prior to immunodetection using GC1 antiserum. *Arrows* point to insulin granules revealing labeling observed with both preimmune (*B*) and GC1 antiserum (*A*). *Bar*, 200 nm in *A* and *B*, 180 nm in *C* and *D*.

and Mitotracker signals superimposed, revealing mitochondrial localization of the newly identified protein. However, resolution obtained with immunofluorescence did not allow ultrastructural localization within mitochondria, *i.e.* mitochondrial matrix *versus* inner or outer mitochondrial membranes.

In this perspective, electron microscopy analysis was performed to nail down GC1 localization within cell compartments. INS-1E sections incubated with GC1 antiserum revealed consistent labeling of numerous mitochondria (Fig. 3*A*), which was restricted to the inner mitochondrial membrane and/or the matrix. We also observed staining within insulin secretory granules and questioned its specificity. Omission of the first antibody (data not shown) and incubation of sections with the preimmune serum (Fig. 3*B*) abolished mitochondrial labeling, although secretory granule labeling persisted. This indicates the specificity of the GC1 antiserum toward mitochondrial localization (Fig. 3*B*). Similar observations were made in mitochondria-enriched INS-1E sections (Fig. 3*C*). Down-regulation of GC1 by adenovirus-mediated shRNA (AdshGC1) markedly reduced anti-GC1 signals in cells analyzed by electron microscopy (Fig. 3*D*).

NAD(P)H Measurements and Mitochondrial Membrane Potential—In β-cells, glucose-induced increases in NAD(P)H are mainly derived from mitochondrial activation. Exposure of control INS-1E cells to stimulatory 15 mM glucose increased NAD(P)H levels (Fig. 4*A*). In cells transduced with GC1shRNA construct glucose-induced elevations of NAD(P)H were not modified as both Empty and AdshGC1 exhibited the same profile. To determine whether overall mitochondrial activation would be affected by GC1 down-regulation, we measured mitochondrial membrane potential. In control cells transduced with the Empty virus, mitochondrial membrane was hyperpolarized by raising the glucose from basal 2.5 to 15 mM (Fig. 4*B*). Further addition of the protonophore FCCP (1 μM) resulted in a rapid depolarization, reflecting dissipation of the proton gradient. A similar profile was observed in cells transduced with the GC1shRNA construct. Glycolysis can be bypassed by the use of

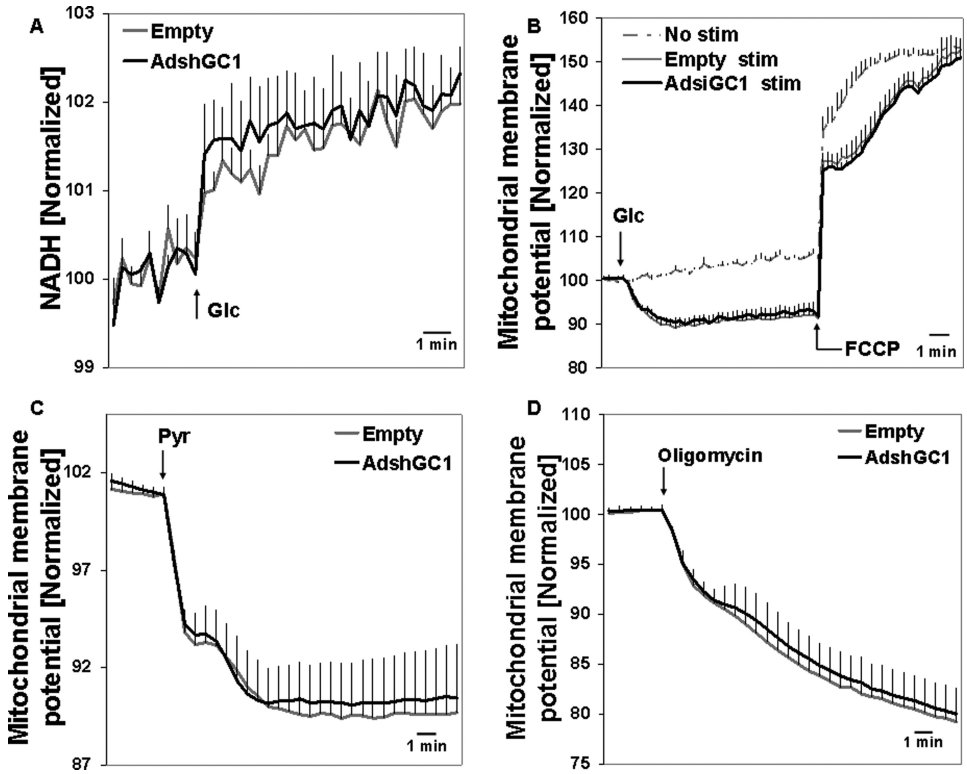

FIGURE 4. **Effect of GC1 down-regulation on NAD(P)H generation and mitochondrial membrane potential.** INS-1E cells were transduced with Empty adenovirus as control or AdshGC1 to down-regulate GC1 and used 4 days later. *A,* NAD(P)H autofluorescence was monitored in INS-1E-transduced cells that were stimulated with 15.5 mM glucose for 10 min. Data are the mean ± S.E. of five independent experiments. The mitochondrial membrane potential was monitored using rhodamine-123 fluorescence in cells that were first exposed to basal 2.5 mM glucose, and mitochondrial membrane hyperpolarization was then elicited by addition of 15.5 mM glucose (*B*), 2 mM pyruvate (*Pyr*) (*C*), and 1 μg/ml oligomycin (*D*). Control depolarization was assessed with the uncoupler FCCP. Values are means ± S.E. of three independent experiments. *No stim*, no stimulation.

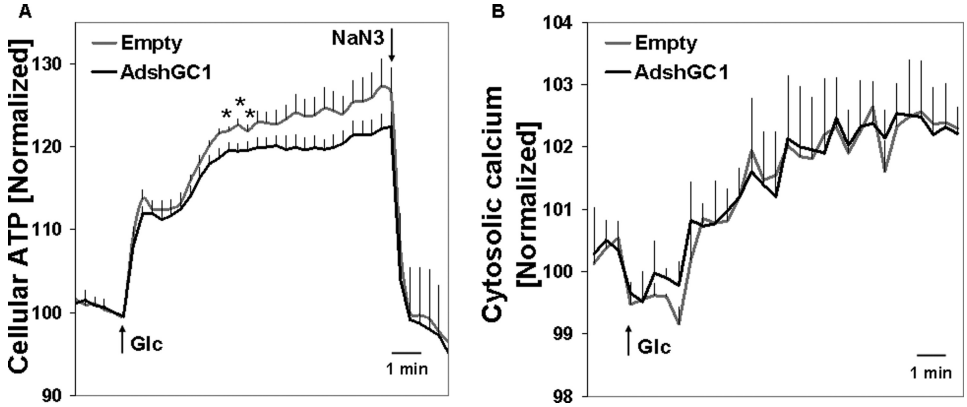

FIGURE 5. **Effect of GC1 down-regulation on cellular ATP and cytosolic calcium levels.** *A,* cytosolic ATP, assessed by bioluminescence, was monitored in transduced cells expressing luciferase. Cells were stimulated with 15 mM glucose (*Glc*) and for 20 min 2 mM NaN3 was added as an inhibitor of the respiratory chain. Values are means ± S.E. of five independent experiments. *B,* cytosolic calcium concentrations were monitored as Fura-2 fluorescence. Calcium rises were induced by switching from basal 2.5 mM to stimulatory 15 mM glucose. Values are means ± S.E. of three independent experiments. *, $p < 0.05$ *versus* Empty.

the mitochondrial substrate pyruvate. Stimulation of mitochondrial hyperpolarization with 1 mM pyruvate revealed no difference between Empty and AdshGC1-transduced cells (Fig. 4*C*). In addition, we tested the effect of the mitochondrial F_1F_0-ATP synthase inhibitor oligomycin (1 μg/ml). Amplitudes and kinetics of the response to oligomycin were similar in Empty and AdshGC1-transduced cells (Fig. 4*D*), indicating preserved coupling between proton transport and ATP generation. These results indicate that the activation of the electron transport chain was not modified by GC1 silencing.

Cellular ATP and Cytosolic Calcium Levels—Cellular ATP generation, monitored in cells expressing luciferase, showed a sustained increase when raising glucose from 2.5 to 15 mM (Fig. 5*A*). This increase was observed in both control and cells treated with the GC1shRNA construct, despite slight transient reduction in GC1 knocked down cells.

Elevation of cytosolic Ca^{2+} is necessary for stimulation of insulin exocytosis, although it does not account for the full development of the glucose response. We checked if GC1 down-regulation would affect glucose-evoked cytosolic Ca^{2+} rises. As shown in Fig. 5*B*, this was not the case as both control and AdshGC1-treated cells similarly responded to 15 mM glucose stimulation by raising cytosolic free Ca^{2+} to similar levels. Taken together, these results show that GC1 silencing did not affect mitochondrial activation as a whole and preserved the triggering pathway leading to Ca^{2+} elevation.

Glutamate Transport Activity—We tested the activity of the mitochondrial glutamate carrier GC1 in mitochondrial extracts from INS-1E cells by assaying the rate of the [^{14}C]glutamate/glutamate exchange in reconstituted liposomes (10). As shown in Fig. 6*A*, the uptake of radioactive L-glutamate in liposomes reconstituted with mitochondrial extract from AdshGC1-transduced cells was markedly reduced as compared with liposomes reconstituted with the mitochondrial extract from Empty control cells (17.6 ± 2.4 *versus* 34.0 ± 4.0 nmol of glutamate/mg of protein, respectively, $p < 0.001$).

Because glutamate/glutamate exchange can also be catalyzed by the mitochondrial aspartate/glutamate carrier (12, 36), we measured the rates of glutamate/aspartate and aspartate/aspartate exchanges, which are solely mediated by aspartate/glutamate carrier, under the same experimental conditions. In liposomes reconstituted with mitochondrial extracts from GC1shRNA construct and control cells, the [^{14}C]glutamate/aspartate exchange was 5.7 ± 0.8 and 6.0 ± 0.7 nmol/mg protein, respectively (Fig. 6*B*). In the same

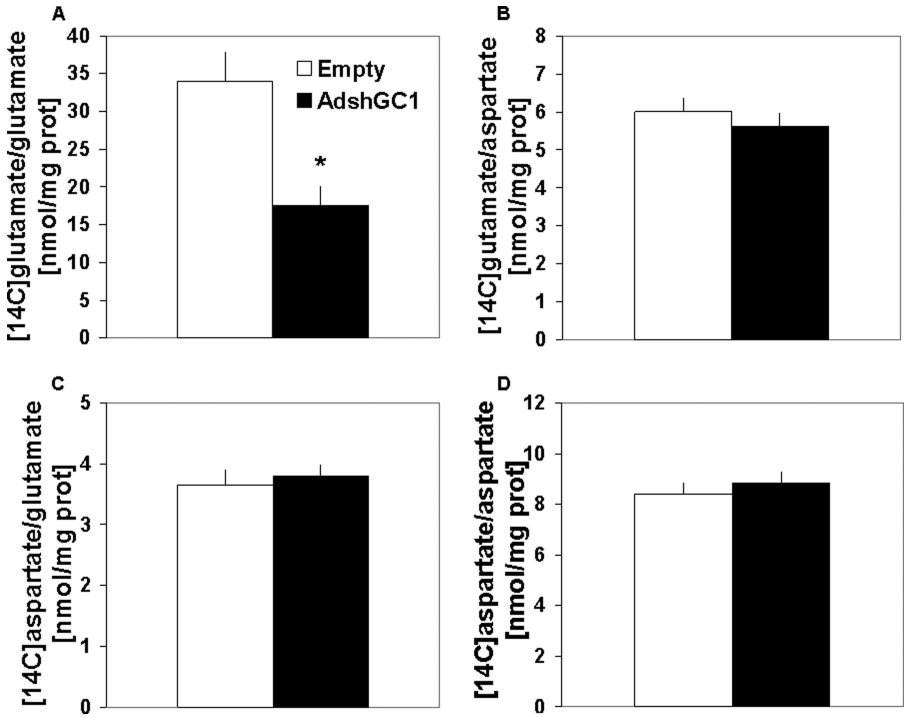

FIGURE 6. **Glutamate transport activity in INS-1E cells with down-regulation of GC1.** Glutamate and aspartate transport activities were assayed in reconstituted liposomes of mitochondrial extracts derived from INS-1E cells transduced 4 days before the experiment with control Empty adenovirus (*white bars*) or AdshGC1 (*black bars*) to down-regulate GC1. Transport was started by adding 1 mM [^{14}C]glutamate (*A* and *B*) or 0.05 mM [^{14}C]aspartate (*C* and *D*) to reconstituted liposomes containing 20 mM glutamate (*A* and *C*) or 20 mM aspartate (*B* and *D*). The reaction time was 3 min. Data are means ± S.E. from five independent experiments performed in triplicate. *, $p < 0.001$ *versus* Empty control, one-way analysis followed by Bonferroni *t* test.

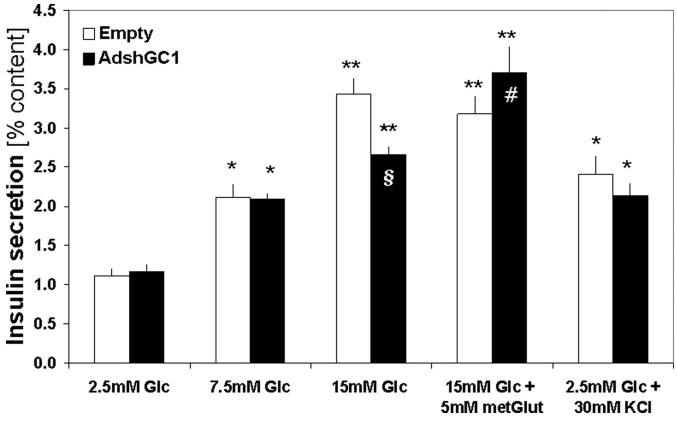

FIGURE 7. **Insulin secretion in INS-1E cells with down-regulation of GC1.** INS-1E cells were transduced with Empty adenovirus as control or AdshGC1 to down-regulate GC1 and used 4 days later. Insulin secretion was measured over a 30-min incubation period at basal 2.5 mM, intermediate 7.5 mM, and stimulatory 15 mM glucose (*Glc*) concentrations. Provision of cell-permeant glutamate was performed at 15 mM glucose by the addition of 5 mM dimethyl glutamate (*metGlut*). Non-nutrient insulin release was tested at 30 mM KCl in the presence of basal 2.5 mM glucose. Values are means ± S.E. *, $p < 0.05$; **, $p < 0.001$ *versus* basal glucose; §, $p < 0.005$ *versus* corresponding control (Empty virus); #, $p < 0.005$ *versus* AdshGC1 15 mM glucose; one-way analysis followed by Bonferroni *t* test.

liposomes, the [^{14}C]aspartate/aspartate exchange was 8.0 ± 1.4 and 7.7 ± 1.3 nmol/mg protein, respectively (Fig. 6*D*). Furthermore, the [^{14}C]aspartate/glutamate exchange was 3.8 ± 0.2 and 3.7 ± 0.2, respectively (Fig. 6*C*). Therefore, the values of the glutamate/aspartate and aspartate/aspartate exchanges are similar between AdshGC1-transduced and control cells in contrast to the values of the glutamate/glutamate exchange.

Effects of GC1 Down-regulation on Insulin Secretion in INS-1E β-Cells—As shown in Fig. 7, INS-1E cells were assayed for secretory responses 4 days after adenoviral transduction. Cells were incubated for a 30-min stimulatory period at basal, intermediate, and high glucose concentrations (2.5, 7.5, and 15 mM glucose). Non-nutrient induced secretion was stimulated by depolarizing concentrations of KCl (30 mM KCl at basal 2.5 mM glucose). The secretory responses in control conditions revealed expected glucose dose response with a 3.1-fold increase upon 15 mM glucose concentrations compared with basal release ($p < 0.001$). In cells treated with the GC1shRNA, there were no differences at basal or intermediate glucose levels. However, the response to 15 mM glucose was reduced by 23% compared with control INS-1E cells ($p < 0.005$). The response to KCl measured in control cells (2.2-fold, $p < 0.05$) was similar in GC1shRNA-treated cells. These results showed that reduced GC1 expression blunted insulin secretion evoked by optimal glucose concentration.

To test if the observed reduction of the secretory responses could be attributed to lower provision of glutamate to the cytosolic compartment, we tested glucose-stimulated insulin secretion in cells loaded with exogenous glutamate in the form of a cell membrane-permeable precursor (Fig. 7). Addition of diemethyl glutamate is known to potentiate the secretory response at intermediate glucose concentrations, although it is not additive to the action of optimal glucose (20). The presence of dimethyl glutamate (5 mM) restored the secretory response evoked by 15 mM glucose in cells silenced for GC1 ($p < 0.005$). These data show that direct modifications of cellular glutamate pools, contributed by GC1, impact on glucose-stimulated insulin secretion (Fig. 7).

Effects of GC1 Down-regulation on Insulin Secretion in Isolated Rat Islets—In accordance with mRNA analysis (Fig. 1*A*), GC1 was expressed at the protein level in rat islets and efficiently down-regulated following treatment with AdshGC1 adenovirus (Fig. 8*A*). Similarly to INS-1E cells, knockdown of GC1 did not inhibit glucose-induced mitochondrial hyperpolarization (Fig. 8*B*).

Kinetics of insulin secretion profiles were determined by performing perifusion experiments on pancreatic islets transduced 4 days prior to analysis with either Empty or GC1shRNA viruses (Fig. 8*C*). Control islets exhibited characteristic biphasic response to 16.7 mM glucose with a transient 8.0-fold increase in insulin secretion when switching from basal to high glucose, followed by sustained secretory response. AdshGC1 trans-

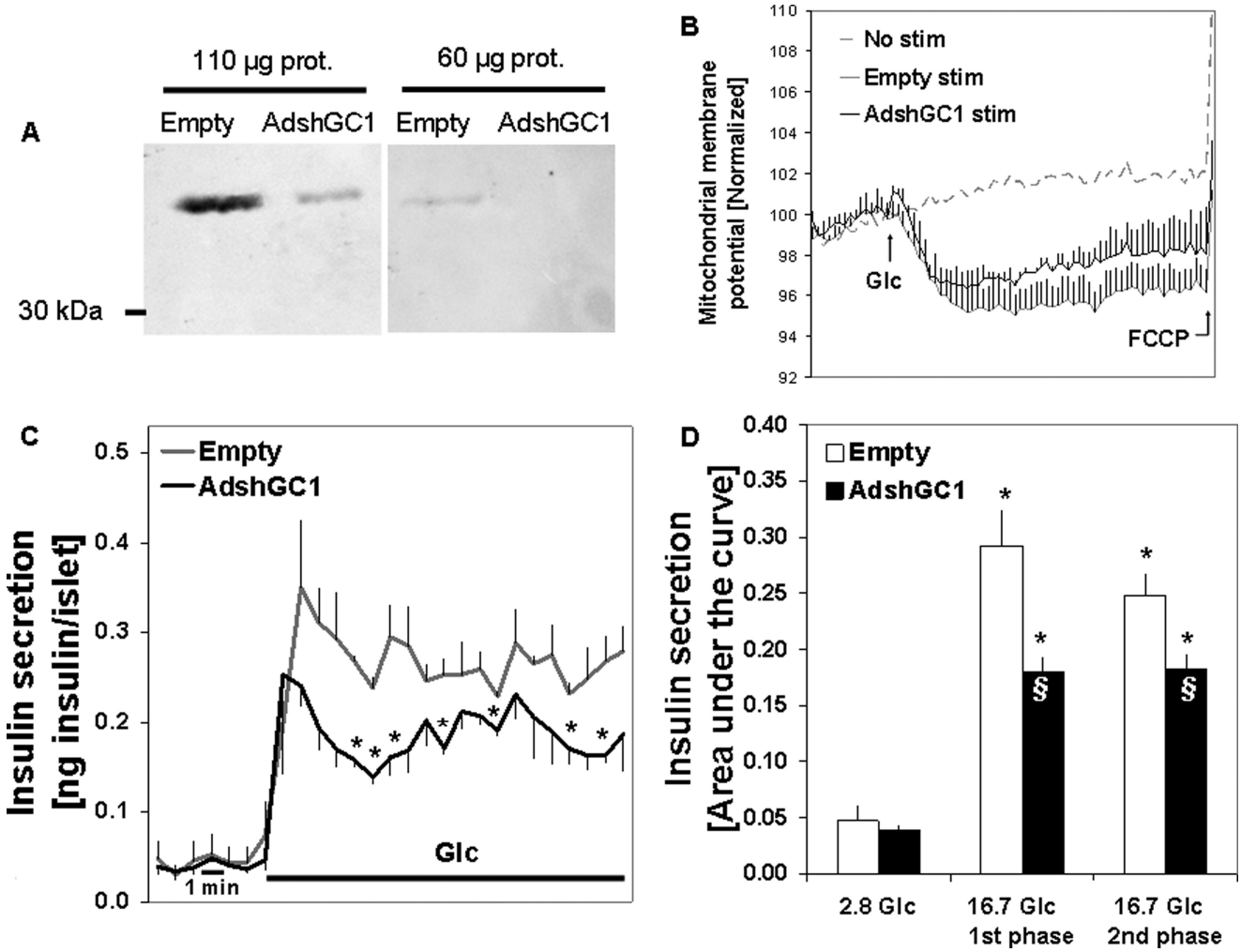

FIGURE 8. **Effects of GC1 down-regulation in isolated rat islets.** Isolated rat islets were transduced with Empty adenovirus as control or AdshGC1 to down-regulate GC1 and used 4 days later. *A,* immunoblot analysis of GC1 expression in isolated islets following SDS-PAGE 15% protein separation using 110 and 60 μg of proteins per lane prepared from two separate experiments (three in total). *B,* mitochondrial membrane potential was monitored using rhodamine-123 fluorescence in isolated islets stimulated with 16.7 mM glucose (*Glc*) for 10 min and then depolarized with the uncoupler FCCP. Values are means ± S.E. of three independent experiments. *C,* insulin secretion profiles were determined by perifusion in response to stimulatory glucose. Transduced islets were perifused with basal 2.8 mM glucose for 15 min and then stimulated with 16.7 mM glucose for 20 min. Data are means ± S.E. of three independent experiments. *, $p < 0.05$ *versus* control (Empty virus) for corresponding time points, analyzed by Student's *t* test. *D,* area under the curve derived from data shown in *C* and normalized per min. The secretory profile was divided into three time frames as follows: basal (2.8 Glc), first phase (first 5-min period following exposure to 16.7 mM Glc), and second phase (from min-6 onward following exposure to 16.7 mM Glc). *, $p < 0.001$ *versus* basal; §, $p < 0.05$ *versus* corresponding control (Empty virus).

duced islets responded to stimulatory glucose, although the amplitude of the secretory response was blunted during both first (−25%, $p < 0.05$) and second phases (−33%, $p < 0.05$), see Fig. 8*D*. These results are consistent with those obtained in the β-cell line INS-1E, *i.e.* GC1 knockdown reduces glucose-stimulated insulin secretion but does not affect basal release.

DISCUSSION

This study ascribes for the first time a physiological role to the mitochondrial glutamate carrier GC1. GC1 (SLC25A22) was previously reported to be expressed at high levels in brain, liver, and pancreas (10). Here, we show that GC1 is expressed in pancreatic islets and insulin-secreting β-cells as assessed by both immunoblotting and immunohistochemistry. Ultrastructural analysis showed that the GC1 glutamate transporter is localized in mitochondria of the INS-1E β-cells. In particular, the distribution of the immunolabeling observed by electron microscopy indicated a matrix and/or inner membrane location of the transporter, consistent with the position of the immunogenic epitope in a matrix loop of GC1. The level of labeling was not high, in agreement with the limited levels of the cognate protein, a hallmark of mitochondrial carriers (38). Silencing of the protein, mediated by shRNA, markedly reduced GC1 expression. Bioinformatics analysis revealed that the sequence cloned from β-cells qualifies as a member of the mitochondrial solute carrier family SLC25.

Silencing of GC1 reduced glutamate transport, although it did not affect electron transport chain as judged by a lack of effect on mitochondrial membrane potential. This suggests that activation of the electron transport chain secondary to glucose metabolism is not dependent on glutamate transport through the mitochondrial membrane. Importantly, knockdown of GC1 inhibited the insulin secretion stimulated by optimal glucose concentrations, although the triggering

pathway leading to Ca^{2+} elevation was preserved. The degree of inhibition of glucose-induced exocytosis was similar in INS-1E β-cells and pancreatic islets, *i.e.* in the range of 30% (23–33%, respectively). This is reminiscent of inhibition reported previously in INS-1E cells and rat islets secondary to overexpression of glutamate decarboxylase, used as a tool to reduce cytosolic glutamate levels (39). Glutamate decarboxylase overexpression blunted glucose-induced glutamate rise and inhibited the secretory response to high glucose by 31% in perifused rat islets (39). More recently, we generated and characterized $\beta Glud1^{-/-}$ transgenic mice with conditional β-cell-specific deletion of the mitochondrial enzyme glutamate dehydrogenase (22). Glutamate dehydrogenase knock-out inhibited glucose-stimulated insulin secretion by about 40%, showing that glutamate pathway is essential for the full development of the secretory response, being sensitive in the upper range of the physiological glucose concentrations (22).

Taken as a whole, past and present data indicate the quantitative contribution of glutamate in the secretory response. In agreement with these cell-based studies, transgenic mice with targeted overexpression of glutamate decarboxylase in the β-cells are glucose-intolerant, and their islets exhibit impaired glucose-stimulated insulin secretion (40). Of note, using either (i) glutamate decarboxylase overexpression to reduce the cytosolic glutamate pool (39), (ii) deletion of the glutamate-forming enzyme glutamate dehydrogenase (22), and (iii) GC1 knockdown to inhibit glutamate transfer between mitochondria and cytoplasm (present data), only high glucose-induced insulin release is lowered. In contrast, basal release, stimulation with intermediate glucose, and the response to the Ca^{2+}-raising agent KCl are all preserved. Enlargement of the cytosolic glutamate pool, contributed by mitochondrial metabolism, might then serve as an amplifying messenger over the Ca^{2+} signal at high glucose levels.

To date, although the role of glutamate is debated (17), several mechanisms of action have been proposed for glutamate as a factor implicated in the control of insulin secretion. Among them, there is evidence for glutamate being taken up by secretory granules (19, 20), an observation correlating with expression of the vesicular glutamate transporters VGLUT1 and VGLUT2 in insulin-secreting cells (41). Once inside the secretory granule, glutamate could induce pH changes as reported in secretory vesicles from pancreatic β-cells (42) and/or activate metabotropic glutamate receptors mGlu5 that have been shown to be expressed in secretory granules, thereby mediating insulin release (43). Alternative mechanisms for glutamate action in insulin-secreting cells include activation of acetyl-CoA carboxylase (44) and inhibition of protein phosphatase enzymatic activities (45), as reversible protein phosphorylation/dephosphorylation cycles have been shown to play a role in the rate of insulin exocytosis (46). All these proposed mechanisms of action require permissive levels of glutamate to be reached in the cytosolic compartment.

Direct specific inhibition of glutamate transport across the inner mitochondrial membrane decreased the efficiency of insulin exocytosis in response to glucose. Noteworthy, both first and second phases of the secretory response were reduced upon GC1 silencing (Fig. 8). The amplifying pathway was originally considered as second phase-specific. However, this paradigm has been recently revised, and amplifying signals are now thought to be implicated in the first and second phases, acting as additive signals on top of the triggering pathway (47). Stimulation of β-cells with high glucose might result in rapid saturation of the respiratory chain (48), favored both by important glycolytic capacity because of high K_m glucokinase and by low lactate release, thereby driving most of glucose catabolic products into mitochondria. The resulting massive activation favors generation of mitochondrial products, such as citrate (49), glutamate (50), GTP (51), and NADH (52). Saturated electron transport chain would then promote export of metabolites out of the mitochondria, a phenomenon well described in β-cells and compensated by important activity of anaplerotic pathways (11, 53). Such mechanisms could signal high nutritional state to the β-cell to adjust the rate of insulin release to levels greater than the sole contribution of Ca^{2+}-induced triggering pathway.

To conclude, this study identifies a new component of the machinery responsible for proper control of insulin secretion. It is remarkable that very little is known about mitochondrial solute carriers, in particular regarding those responsible for the transport of metabolites. Here, the glutamate carrier GC1 is assigned a physiological function, *i.e.* the control of insulin secretion upon elevated glucose stimulation.

Acknowledgments—We thank Gaelle Chaffard, Clarissa Bartley, and Asllan Gjinovci for expert technical assistance.

REFERENCES

1. Palmieri, F. (2004) *Pflugers Arch.* **447,** 689–709
2. Palmieri, F. (2008) *Biochim. Biophys. Acta* **1777,** 564–578
3. Arco, A. D., and Satrústegui, J. (2005) *Cell. Mol. Life Sci.* **62,** 2204–2227
4. Satrústegui, J., Pardo, B., and Del Arco, A. (2007) *Physiol. Rev.* **87,** 29–67
5. Agrimi, G., Di Noia, M. A., Marobbio, C. M., Fiermonte, G., Lasorsa, F. M., and Palmieri, F. (2004) *Biochem. J.* **379,** 183–190
6. Dolce, V., Scarcia, P., Iacopetta, D., and Palmieri, F. (2005) *FEBS Lett.* **579,** 633–637
7. Fiermonte, G., De Leonardis, F., Todisco, S., Palmieri, L., Lasorsa, F. M., and Palmieri, F. (2004) *J. Biol. Chem.* **279,** 30722–30730
8. Floyd, S., Favre, C., Lasorsa, F. M., Leahy, M., Trigiante, G., Stroebel, P., Marx, A., Loughran, G., O'Callaghan, K., Marobbio, C. M., Slotboom, D. J., Kunji, E. R., Palmieri, F., and O'Connor, R. (2007) *Mol. Biol. Cell* **18,** 3545–3555
9. Molinari, F., Raas-Rothschild, A., Rio, M., Fiermonte, G., Encha-Razavi, F., Palmieri, L., Palmieri, F., Ben-Neriah, Z., Kadhom, N., Vekemans, M., Attie-Bitach, T., Munnich, A., Rustin, P., and Colleaux, L. (2005) *Am. J. Hum. Genet.* **76,** 334–339
10. Fiermonte, G., Palmieri, L., Todisco, S., Agrimi, G., Palmieri, F., and Walker, J. E. (2002) *J. Biol. Chem.* **277,** 19289–19294
11. Frigerio, F., Casimir, M., Carobbio, S., and Maechler, P. (2008) *Biochim. Biophys. Acta* **1777,** 965–972
12. Rubi, B., del Arco, A., Bartley, C., Satrustegui, J., and Maechler, P. (2004) *J. Biol. Chem.* **279,** 55659–55666
13. Joseph, J. W., Jensen, M. V., Ilkayeva, O., Palmieri, F., Alárcon, C., Rhodes, C. J., and Newgard, C. B. (2006) *J. Biol. Chem.* **281,** 35624–35632
14. Maechler, P., Carobbio, S., and Rubi, B. (2006) *Int. J. Biochem. Cell Biol.* **38,** 696–709
15. Ashcroft, F. M. (2005) *J. Clin. Invest.* **115,** 2047–2058
16. Yang, S. N., and Berggren, P. O. (2005) *Am. J. Physiol. Endocrinol. Metab.* **288,** E16–E28
17. Henquin, J. C. (2000) *Diabetes* **49,** 1751–1760
18. Wollheim, C. B., and Maechler, P. (2002) *Diabetes* **51,** S37–S42

19. Høy, M., Maechler, P., Efanov, A. M., Wollheim, C. B., Berggren, P. O., and Gromada, J. (2002) *FEBS Lett.* **531,** 199–203
20. Maechler, P., and Wollheim, C. B. (1999) *Nature* **402,** 685–689
21. Maechler, P., Gjinovci, A., and Wollheim, C. B. (2002) *Diabetes* **51,** S99–S102
22. Carobbio, S., Frigerio, F., Rubi, B., Vetterli, L., Bloksgaard, M., Gjinovci, A., Pournourmohammadi, S., Herrera, P. L., Reith, W., Mandrup, S., and Maechler, P. (2009) *J. Biol. Chem.* **284,** 921–929
23. Fahien, L. A., MacDonald, M. J., Kmiotek, E. H., Mertz, R. J., and Fahien, C. M. (1988) *J. Biol. Chem.* **263,** 13610–13614
24. Li, C., Matter, A., Kelly, A., Petty, T. J., Najafi, H., MacMullen, C., Daikhin, Y., Nissim, I., Lazarow, A., Kwagh, J., Collins, H. W., Hsu, B. Y., Nissim, I., Yudkoff, M., Matschinsky, F. M., and Stanley, C. A. (2006) *J. Biol. Chem.* **281,** 15064–15072
25. Sener, A., Somers, G., Devis, G., and Malaisse, W. J. (1981) *Diabetologia* **21,** 135–142
26. Merglen, A., Theander, S., Rubi, B., Chaffard, G., Wollheim, C. B., and Maechler, P. (2004) *Endocrinology* **145,** 667–678
27. Carobbio, S., Ishihara, H., Fernandez-Pascual, S., Bartley, C., Martin-Del-Rio, R., and Maechler, P. (2004) *Diabetologia* **47,** 266–276
28. Kennedy, E. D., Maechler, P., and Wollheim, C. B. (1998) *Diabetes* **47,** 374–380
29. Maechler, P., Jornot, L., and Wollheim, C. B. (1999) *J. Biol. Chem.* **274,** 27905–27913
30. Bosco, D., Meda, P., Morel, P., Matthey-Doret, D., Caille, D., Toso, C., Bühler, L. H., and Berney, T. (2005) *Diabetologia* **48,** 1523–1533
31. Scheiermann, C., Meda, P., Aurrand-Lions, M., Madani, R., Yiangou, Y., Coffey, P., Salt, T. E., Ducrest-Gay, D., Caille, D., Howell, O., Reynolds, R., Lobrinus, A., Adams, R. H., Yu, A. S., Anand, P., Imhof, B. A., and Nourshargh, S. (2007) *Science* **318,** 1472–1475
32. Maechler, P., Wang, H., and Wollheim, C. B. (1998) *FEBS Lett.* **422,** 328–332
33. Rubí, B., Ljubicic, S., Pournourmohammadi, S., Carobbio, S., Armanet, M., Bartley, C., and Maechler, P. (2005) *J. Biol. Chem.* **280,** 36824–36832
34. Palmieri, L., Vozza, A., Hönlinger, A., Dietmeier, K., Palmisano, A., Zara, V., and Palmieri, F. (1999) *Mol. Microbiol.* **31,** 569–577
35. Palmieri, F., Indiveri, C., Bisaccia, F., and Iacobazzi, V. (1995) *Methods Enzymol.* **260,** 349–369
36. Palmieri, L., Pardo, B., Lasorsa, F. M., del Arco, A., Kobayashi, K., Iijima, M., Runswick, M. J., Walker, J. E., Saheki, T., Satrústegui, J., and Palmieri, F. (2001) *EMBO J.* **20,** 5060–5069
37. Puigserver, P., Herron, D., Gianotti, M., Palou, A., Cannon, B., and Nedergaard, J. (1992) *Biochem. J.* **284,** 393–398
38. Palmieri, F. (1994) *FEBS Lett.* **346,** 48–54
39. Rubi, B., Ishihara, H., Hegardt, F. G., Wollheim, C. B., and Maechler, P. (2001) *J. Biol. Chem.* **276,** 36391–36396
40. Shi, Y., Kanaani, J., Menard-Rose, V., Ma, Y. H., Chang, P. Y., Hanahan, D., Tobin, A., Grodsky, G., and Baekkeskov, S. (2000) *Am. J. Physiol. Endocrinol. Metab.* **279,** E684–E694
41. Bai, L., Zhang, X., and Ghishan, F. K. (2003) *Am. J. Physiol. Gastrointest. Liver Physiol.* **284,** G808–G814
42. Eto, K., Yamashita, T., Hirose, K., Tsubamoto, Y., Ainscow, E. K., Rutter, G. A., Kimura, S., Noda, M., Iino, M., and Kadowaki, T. (2003) *Am. J. Physiol. Endocrinol. Metab.* **285,** E262–E271
43. Storto, M., Capobianco, L., Battaglia, G., Molinaro, G., Gradini, R., Riozzi, B., Di Mambro, A., Mitchell, K. J., Bruno, V., Vairetti, M. P., Rutter, G. A., and Nicoletti, F. (2006) *Mol. Pharmacol.* **69,** 1234–1241
44. Kowluru, A., Chen, H. Q., Modrick, L. M., and Stefanelli, C. (2001) *Diabetes* **50,** 1580–1587
45. Lehtihet, M., Honkanen, R. E., and Sjöholm, A. (2005) *Biochem. Biophys. Res. Commun.* **328,** 601–607
46. Jones, P. M., and Persaud, S. J. (1998) *Endocr. Rev.* **19,** 429–461
47. Henquin, J. C., Ravier, M. A., Nenquin, M., Jonas, J. C., and Gilon, P. (2003) *Eur. J. Clin. Invest.* **33,** 742–750
48. Antinozzi, P. A., Ishihara, H., Newgard, C. B., and Wollheim, C. B. (2002) *J. Biol. Chem.* **277,** 11746–11755
49. Farfari, S., Schulz, V., Corkey, B., and Prentki, M. (2000) *Diabetes* **49,** 718–726
50. Broca, C., Brennan, L., Petit, P., Newsholme, P., and Maechler, P. (2003) *FEBS Lett.* **545,** 167–172
51. Kibbey, R. G., Pongratz, R. L., Romanelli, A. J., Wollheim, C. B., Cline, G. W., and Shulman, G. I. (2007) *Cell Metab.* **5,** 253–264
52. Rocheleau, J. V., Head, W. S., and Piston, D. W. (2004) *J. Biol. Chem.* **279,** 31780–31787
53. Schuit, F., De Vos, A., Farfari, S., Moens, K., Pipeleers, D., Brun, T., and Prentki, M. (1997) *J. Biol. Chem.* **272,** 18572–18579